

# Oblique superinsulator nature of the pseudogap state

M. C. Diamantini,<sup>1</sup> C. A. Trugenberger,<sup>2</sup> and V. M. Vinokur<sup>3,4</sup>

<sup>1</sup>NiPS Laboratory, INFN and Dipartimento di Fisica e Geologia,  
University of Perugia, via A. Pascoli, I-06100 Perugia, Italy

<sup>2</sup>SwissScientific Technologies SA, rue du Rhone 59, CH-1204 Geneva, Switzerland

<sup>3</sup>Materials Science Division, Argonne National Laboratory, 9700 S. Cass Ave, Argonne, IL 60439, USA

<sup>4</sup>Consortium for Advanced Science and Engineering (CASE) University of Chicago, 5801 S Ellis Ave, Chicago, IL 60637, USA

At present, a general description of the experimentally observed universal features of the pseudogap phase and their connection with HTS is still lacking. Here we construct a unifying effective field theory capturing the universal characteristics of HTS materials and explaining the observed phase diagram. We show that the pseudogap state is a phase where a charged magnetic monopole condensate realizes oblique confinement of Cooper pairs in form of an oblique version of a superinsulator. We demonstrate that the HTS phase diagram is dominated by a tricritical point (TCP) at which the first order transition between a fundamental Cooper pair condensate and a charged magnetic monopole condensate merges with continuous superconductor-normal metal and superconductor-pseudogap state transitions. The universality of the HTS phase diagram reflects a unique topological mechanism of competition between the magnetic monopole condensate, inherent to antiferromagnetic-order-induced Mott insulators and the Cooper pair condensate. Our findings provide a topological reason for the high critical temperature

## INTRODUCTION

The key to unraveling the nature of high-temperature superconductivity (HTS) lies in resolving the enigma of the pseudogap state [1–5]. The pseudogap state that appears in the underdoped region [5] forms a distinct thermodynamic phase characterized by nematicity [3], temperature-quadratic resistive behavior, and magnetoelectric effects [1]. Strong electron interactions in HTS, resulting in strong Cooper pairing [5], localize the very-low-doped antiferromagnetic state into a Mott insulator [1, 6, 7]. Further doping, i.e. adding further  $p$  holes per Cu atom, turns the electrons itinerant. Thus, the superconductivity dome forms in the  $p \approx 0.05 \div 0.3$  interval, followed by a Fermi liquid at higher doping, see phase diagram in Fig. 1. The puzzling pseudogap (PG) state, remaining elusive despite two decades of extensive debate, emerges in the underdoped region. Above the temperature  $T^*$ , associated with the onset of the PG, a metallic sheet resistance linear in temperature,  $R_\square \propto T$ , is observed. Below some lower temperature,  $T^{**} < T^*$ , a distinct switch to a quadratic dependence  $R_\square \propto T^2$  occurs, holding down till superconducting fluctuations set in, see [1, 6] and references therein. The PG full switch at  $T=T^{**}$  is accompanied by the nematic phase transition and emergence of the magnetoelectric (Kerr) effect, see [3, 7–9] and references therein, evidencing that the PG state is a distinct thermodynamic phase. Recent shot noise measurements deep in the PG region detected pairing of the charge carriers [4]. Finally, the evolution from Mott insulator at  $p = 0$  to superconductivity upon increasing  $p$ , suggests a quantum superconductor-insulator transition (SIT) between two distinct quantum orders [10]. These orders are supposed to coexist within the superconducting dome. The putative transition point is at  $p^*$  where the  $T^*(p)$  line continued into the dome hits the  $p$ -axis, see Fig. 1. This quantum critical point (QCP) is often viewed as a dominant ingredient of the HTS phase diagram.

Taking this idea as our starting point, let us recall that, in two dimensions (2D), the SIT, see [11] for a review, may occur via intermediate quantum phase transitions across an intervening Bose metal state [12–14]. The latter has been identified [15] as a bosonic topological insulator (BTI) [16] in which metallic-like charge transport is mediated by the symmetry-protected edge states [17]. An immediate question is whether the same mechanism arises as well in 3D, where the system comprises more than one superconducting plane (in this respect a BSCCO monolayer [18] is a 3D system) so that Cooper pairs can tunnel between them in the  $c$ -direction. If such a mechanism is realized, the charge carriers are expected to be Cooper pairs, as is indeed seen in experiment [4], but acquire fermionic character due to topological effects confining them to the surface. However, the simplest 3D BTI with no time-reversal symmetry breaking and no topological order has no fermionic surface degrees of freedom [19]. This leads us to conjecture that the PG is associated with the other quantum state appearing in the SIT, namely with the superinsulating state [12, 20]. The electromagnetic response of superinsulators is described by compact QED [21] in the phase where magnetic monopoles [22] form a Bose condensate [23, 24]. Ordinarily, Cooper pairs in a superinsulator are linearly confined by electric strings, which results in an infinite resistance at finite temperatures [25, 26]. This implies that the superinsulation realized in the PG state differs from the standard one, and we turn now to its description.

## RESULTS

The fact that the PG state exhibits magnetoelectric effects [1] brings to the immediate conclusion that its electromagnetic response contains the topological  $\theta$ -term [27] (or the axion term) in the Lagrangian,

$$\mathcal{L}_\theta = \frac{\theta}{32\pi^2} F_\mu \epsilon^{\mu\nu\alpha\beta} F_{\alpha\beta} = \frac{\theta}{4\pi^2} \mathbf{E} \cdot \mathbf{B}, \quad (1)$$

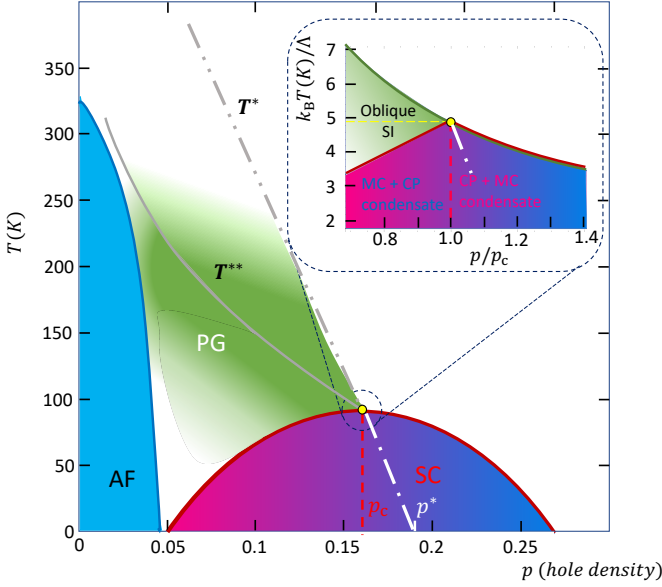


FIG. 1. A sketch of the temperature-doping phase diagram of HTS. The phase diagram presents different phases, including anti-ferromagnetism (blue), superconductivity (purple to dark blue), and pseudogap (green) domains. The dashed grey line at  $T^*$  marks the onset of the pseudogap phase detected by deviation from the linear  $R_0 \propto T$  resistance dependence. The grey dashed-point line,  $T^{**}$ , indicates the emergence of square  $R_0 \propto T^2$  resistance dependence, nematicity, and magnetoelectric effects. The  $p_c$  marks the tricritical point at the dome maximum, and  $p^*$ , where  $T^*$  hits the x-axis, is the position of the putative quantum Mott-insulator-superconductor phase transition at  $T = 0$ . **Inset:** The calculated phase transition lines in the vicinity of the tricritical point.

where  $(\theta/4\pi^2)\delta_{ij}$  represents the pseudoscalar part of the magnetoelectric coupling, or polarizability  $\alpha_{ij} \equiv [\partial M_j / \partial E_i]_{\mathbf{B}=0} \equiv [\partial P_i / \partial B_j]_{\mathbf{E}=0}$ ,  $\mathbf{E}$  and  $\mathbf{B}$  are the electric and magnetic fields,  $\mathbf{P}$  and  $\mathbf{M}$  are the polarization and magnetization, and we use natural units  $c=1$ , with  $c$  being the light velocity in the material,  $\hbar=1$ ,  $\epsilon_0=1$ , Greek letters denote space-time indices and a sum is implied over repeating indices. The  $\theta$ -term, or axial anomaly, is a pure surface term on bounded spaces. On a compact Euclidean torus  $\mathbf{T}^4$ , the integral of the  $\theta$ -term is a topological invariant contributing a factor  $\exp(in\theta)$  to the partition function, hence  $\theta$  is  $2\pi$ -periodic. Since the  $\theta$ -term describes the topological coupling of a vector and a pseudovector field, it is odd under parity and time-reversal symmetries. The values of  $\theta$  compatible with the time-reversal symmetry are thus  $\theta = 0 \pmod{2\pi}$  and  $\theta = \pi \pmod{2\pi}$ .

The phase structure of the compact QED with a  $\theta$ -term (1) has been investigated in a seminal paper by Cardy and Rabinovici [28]. They considered the Euclidean lattice gauge model

$$Z = \sum_{\{n_\mu\}, \{m_\mu\}} \int \mathcal{D}A_\mu e^{-S},$$

$$S = \sum_x \frac{1}{4f^2} (F_{\mu\nu} - 2\pi S_{\mu\nu})^2 + iA_\mu \left( n_\mu + \frac{\theta}{2\pi} m_\mu \right), \quad (2)$$

where  $A_\mu$  is the gauge field,  $F_{\mu\nu}$  the corresponding field strength, the integers  $n_\mu$  and  $m_\mu = (1/2)K_{\mu\alpha\beta}S_{\alpha\beta}$  denote the conserved charge and magnetic monopole currents, respectively, and  $K_{\mu\alpha\beta}$  is the lattice BF operator [12] (see Methods). Present context implies the dimensionless coupling  $f$  to be an effective strength of the Coulomb interaction in the material. Magnetic monopoles are topological excitations arising in the electromagnetic response due to the compact nature of the electromagnetic gauge potential. Equation (2) implies that, in the presence of the topological  $\theta$ -term, magnetic monopoles acquire an electric charge  $\theta/2\pi$  and become *dyons*. This is known as Witten effect [29] and is the sole bulk consequence of a  $\theta$ -term in a compact gauge theory. Having in mind Cooper pairs, we let the unit of charge be  $2e$ . The Dirac quantization condition  $qg/(4\pi\hbar) = n/2$ , where  $q$  and  $g$  are any electric and magnetic charge, with  $n$  an integer [22], then requires the unit of magnetic charge be  $\pi/e$ .

By integrating out the gauge field  $A_\mu$ , one obtains the model formulated solely in terms of charge and monopole currents,

$$Z = \sum_{\{n_\mu\}, \{m_\mu\}} e^{-S},$$

$$S = \sum_x f^2 \left( n_\mu + \frac{\theta}{2\pi} m_\mu \right) \frac{1}{-\nabla^2} \left( n_\mu + \frac{\theta}{2\pi} m_\mu \right) + \frac{\pi^2}{f^2} \sum_x m_\mu \frac{1}{-\nabla^2} m_\mu$$

$$+ i\pi n_\mu \frac{1}{-\nabla^2} K_{\mu\alpha\beta} M_{\alpha\beta}(\mathbf{z})$$

where the integers  $M_{\mu\nu} = (1/2)S_\mu \epsilon_{\mu\nu\alpha\beta} S_{\alpha\beta}$  are such that  $m_\mu = \Delta_\nu M_{\mu\nu}$  ( $S_\mu$  is the lattice shift operator, see Methods). The last term represents the topological interaction between charges and monopoles. When the Dirac quantization condition is satisfied, it falls out of the partition function since it is always an integer multiple of  $2\pi$ , as can be easily seen by representing the conserved charge current as  $n_\mu = K_{\mu\alpha\beta} X_{\alpha\beta}$ , with the gauge conditions  $\Delta_\alpha X_{\alpha\beta} = \Delta_\beta X_{\alpha\beta} = 0$ , so that  $X_{\alpha\beta}$  contains four degrees of freedom as  $n_\mu$ , and using the relation (15) in Methods.

Following [30] and keeping only self-interaction terms, one assigns to particles an action proportional to the length  $N$  of their (Euclidean) world-line, representing a lattice string. As usual in statistical field theory, this Euclidean action is equivalent to the “energy” of an equivalent statistical model in one more spatial dimension, where the coupling constant plays the role of “temperature”. Since the entropy of a lattice string is also proportional to its length, the “free energy” of a particle with the electric charge  $n$  and magnetic charge  $m$  appears as

$$F = \left[ f^2 G(0) \left( n + \frac{\theta}{2\pi} m \right)^2 + \frac{\pi^2}{f^2} G(0) m^2 - \mu \right] N, \quad (4)$$

where  $G(0)$  is the value of the lattice Coulomb potential at coinciding points and  $\mu \approx \ln 7$ , since at each step the non-backtracking string has to choose among 7 possible directions to continue. If the factor  $[\emptyset]$  at  $N$  given by brackets is positive, the free energy is minimal for  $N = 0$ . If, instead, it is negative, the free energy is minimized by  $N = \infty$ . This means

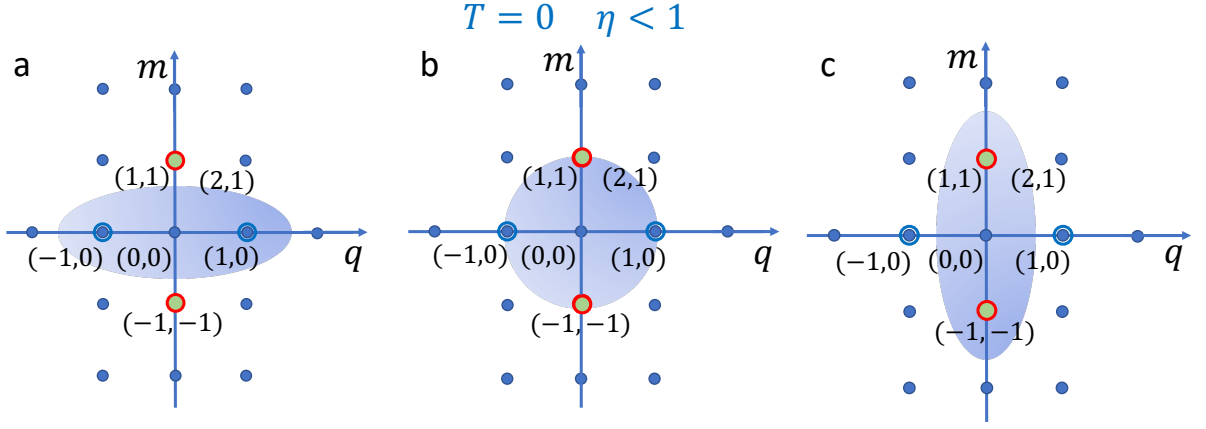


FIG. 2. **The ellipse technique for calculating emerging phases at  $T = 0$  and  $\eta < 1$ .** The  $x$ -axis shows the integer dyonic charges  $q = m + n$ , for  $\theta = 2\pi$ , while the  $y$ -axis lists integer magnetic charges  $m$ . **a:** Superconducting state, where only points  $n = \pm 1$  (electric charge) and  $m = 0$  (blue circles) fall inside the ellipse. **b:** First order phase transition between the superconductor and oblique superinsulator as the ellipse contains both superconducting and dyonic unit charge ( $q = \pm 1, m = \pm 1$ ) integer points (red rim green circles). **c:** Oblique superinsulator phase.

that particles with quantum numbers for which  $[\phi]$  in Eq. (4) is positive are suppressed and exist only as short-lived fluctuations, while particles with quantum numbers for which  $[\phi]$  is negative form Bose condensates. If both Bose condensates are possible, the one with the lowest free energy is stable, but phases may coexist. The condensation condition

$$\eta \frac{f^2}{\pi} \left( n + \frac{\theta}{2\pi} m \right)^2 + \eta \frac{\pi}{f^2} m^2 < 1, \quad (5)$$

where  $\eta = \pi G(0)/\mu$ , describes the interior of a tilted ellipse with semiaxes  $r_n = \sqrt{\pi/f^2} \sqrt{1/\eta}$  and  $r_m = \sqrt{f^2/\pi} \sqrt{1/\eta}$  on an integer lattice of electric and magnetic charges. The quantity  $1/\sqrt{\eta}$  defines the overall scale of the ellipse, while the coupling  $f^2/\pi$  is the ratio between its semiaxes. Varying the coupling  $f$  and angle  $\theta$  leads to complex phase structures consisting of alternating sequences of three possible phases [28], a superconducting phase consisting of a pure charge condensate ( $m=0$ ), a Coulomb phase with no condensate, and an oblique confinement phase, where condensed particles carry both electric and magnetic charges [31].

Seminal reference [28] restricted its analysis to  $\theta \in [0, 2\pi[$  because of the periodicity of the charge spectrum under shifts  $\theta \rightarrow \theta + 2\pi$ . This periodicity is evident in (4) and (5), since the shift  $\theta \rightarrow \theta + 2\pi$  can be compensated by the corresponding shift  $n \rightarrow n - m$ . As a consequence of this restriction, the superconducting and oblique confinement phases can never be adjacent, but are always separated by Coulomb phases [28]. Importantly, however, the correct periodicity is achieved by shifts  $\theta \rightarrow \theta + 4\pi$ . While the charge of dyonic composites is indeed periodic under shifts  $\theta \rightarrow \theta + 2\pi$ , their statistics is not, if charges are bosonic, as has been pointed out in [32]. The statistics of a composite of  $n$  bosonic electric charges and  $m$  magnetic monopoles with  $\theta = 0$  is  $(-1)^{nm}$ , where  $+1$  corresponds to bosons and  $-1$  to fermions [33, 34]. If we turn on the angle  $\theta$ , the total electric charge changes to  $q = n + m\theta/2\pi$  but the statistics remains unchanged [35]. If we compensate

the shift  $\theta \rightarrow \theta + 2\pi$  by the corresponding transformation  $n \rightarrow n - m$ , to leave the total charge unchanged, we change the statistics of the composite by the factor  $(-1)^{m^2}$ , which is not necessarily unity. Only the shift  $\theta \rightarrow \theta + 4\pi$ , accompanied by  $n \rightarrow n - 2m$ , yields the same charge and statistics. Had charges been fermions, then the correct periodicity, indeed, would have been  $\theta \rightarrow \theta + 2\pi$ , but fermions do not Bose condense. This statistical Witten effect [32] is the same reason why strong bosonic topological insulators are also periodic only under shifts  $\theta \rightarrow \theta + 4\pi$ , contrary to fermionic ones [19].

Since the correct periodicity in the angle  $\theta$  is  $4\pi$ , and not  $2\pi$ , the case  $\theta = 2\pi$  is generically different from that with  $\theta = 0$ . For  $\theta = 2\pi$  the  $(n, m)$  lattice is not tilted, but all  $m = \text{const} \neq 0$  lines are shifted in their  $n$ -values with respect to the  $x$ -axis  $m = 0$ , as shown in Fig. 2. Cranking down the coupling  $\pi/f^2$  from high (corresponding to weak Coulomb interactions) to small (corresponding to strong Coulomb interactions) values, first elongates the ellipse along the  $x$ -axis, then passes it through a circle, and, finally, elongates it along the  $y$ -axis. At  $\eta > 1$ , the nearly circles forming at the mid-way contain only the origin of the lattice, which corresponds to the Coulomb insulating phase. At  $\eta < 1$ , instead, the deformation processes from horizontally elongated ellipses containing the lattice point  $(n = 1, m = 0)$  and describing the superconductor, Fig. 2a, through a circle containing both kinds of lattice points, Fig. 2b, to vertically elongated ellipses containing the lattice point  $(n = 0, m = 1)$  and corresponding to the oblique confinement, Fig. 2c. This describes a first-order transition at which the superconducting order and oblique confinement coexist. The particles in both these coexisting condensates carry unit charge, but for the ‘superconducting’ particles the charge is fundamental, while ‘oblique confinement’ carriers acquire charge due to the Witten effect. Since  $G(0) = 0.155$  and  $\mu \approx \ln 7$ , we have  $\eta = 0.25 < 1$ . It is exactly this coexistence regime that is realized, without an intervening normal insulating phase. Upon increasing the temperature, the overall

scale of the ellipse shrinks, see Fig. 3, by the scale factor  $S(T)$  shown in the inset in Fig. 3, see Methods. Thus, lattice points that were within the ellipse at  $T = 0$  fall out as the temperature grows and the system crosses from the under-the-dome superconducting coexistence phase to the pseudogap state and then to a metallic phase as illustrated in Fig. 3.

As we have already mentioned, the realization of a magnetic monopole condensate is a superinsulator [12, 20, 25, 26]. Accordingly, we name the material hosting an oblique confinement phase an *oblique superinsulator*. The numerically computed phase diagram in the vicinity of the tricritical point is shown in the inset in Fig. 1, where we have identified the coupling constant  $\pi/f^2$  with the doping normalized to unity at the  $T_c$  maximum, and values of  $T_c = O(100)$  K are obtained for the cutoff  $\Lambda \approx 2$  Kev, i.e. frequencies  $\approx 1/2$  THz which is of order of the plasma frequency in cuprates. The colored regions mark a charged monopole condensate with the magnetic charge  $\pi/e$ . Accordingly, stable single electrons are forbidden by the Dirac quantization condition, since they would have carried the angular momentum  $1/4$  [22]. In finite systems with a finite density of monopoles this topological obstruction reduces to a finite energy barrier, and single electrons can appear only as short-lived fluctuations with energies above this barrier. Below the superconducting dome (purple), the charged monopole condensate coexists with the fundamental Cooper pair condensate, and the dash-dotted line hitting  $T=0$  axis at  $p=p^*$ , depicts the first-order phase transition. In the overdoped region,  $p/p_{cr} > 1$ , the boundary of the superconducting dome marks the region where the magnetic monopoles cease to exist. Above this phase boundary, the Cooper pairs are free to split into single electrons to form a normal metal. In the underdoped region  $p/p_{cr} < 1$ , the phase boundary marks the vanishing of the fundamental charge condensate. For higher temperatures, only the charged monopole condensate, i.e. the oblique superinsulator, survives. We identify this state as the pseudogap state below the temperature  $T^*$  [1]. In the proposed model, the physics of the high- $T_c$  cuprates is dominated by the *tricritical point* at  $p/p_c = 1$  and  $k_B T_c/\Lambda = 4.9$ , where the first-order transition within the superconducting dome meets two continuous transitions to a normal metal (in the overdoped region) and to the pseudogap state (in the underdoped region). This universal structure is an implication of the presence of the magnetic monopole condensate in cuprates. Furthermore, monopoles ensure that in the underdoped region the charge carriers appear as paired well above  $T_c$  [4]: the out of condensate Cooper pairs are protected from splitting into single electrons by the Dirac quantization condition.

In a superconductor, the electromagnetic response is mediated by photons with mass  $(1/2)\lambda_L^{-2}A_\mu A^\mu$ , leading to the London equations  $j^\mu = \lambda_L^{-2}A_\mu$ . The corresponding electromagnetic response of an oblique superinsulator has been derived in [36, 37]. As in superconductors, the condensate generates a massless mode that combines with the photon to produce a massive excitation. Contrary to superconductors, however, this massless mode is not a scalar representing the phase of the charge order parameter but, rather, the “dual magnetic phase”,

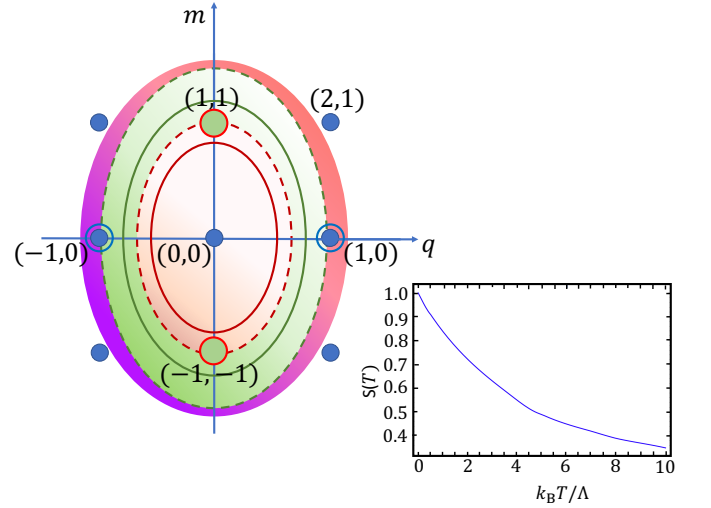


FIG. 3. **Temperature evolution and deconfinement at  $p < p_c$ .** The purple ellipse corresponds to the coexistence of dyonic and superconducting condensates. The green dashed line corresponds to the temperature at which the transition from the superconducting dome to the pseudogap phase occurs. The solid green line corresponds to temperatures at which the pseudogap phase exists. The dashed fire brick line marks the further transition from the pseudogap to a metallic state and the solid fire brick line corresponds to the metallic state. **Inset:** The scaling function  $S(T)$ , see Methods.

embedded into an antisymmetric tensor gauge field  $B_{\mu\nu}$ , with the three-tensor field strength  $H_{\mu\nu\rho} = \partial_\mu B_{\nu\rho} + \partial_\nu B_{\rho\mu} + \partial_\rho B_{\mu\nu}$  invariant under the gauge symmetries of the second kind,  $B_{\mu\nu} \rightarrow B_{\mu\nu} + \partial_\mu \lambda_\nu - \partial_\nu \lambda_\mu$ . Since  $B_{0i}$  are Lagrange multipliers with no time derivatives appearing in the kinetic term  $H_{\mu\nu\rho}$ , and the gauge function  $\lambda_\mu$  is itself defined only up to a derivative, the antisymmetric tensor contains indeed a single degree of freedom. The full electromagnetic response of the oblique superinsulator is

$$\mathcal{L} = -\frac{1}{4f^2} (B_{\mu\nu} + F_{\mu\nu}) (B^{\mu\nu} + F^{\mu\nu}) + \frac{\theta}{32\pi^2} (B_{\mu\nu} + F_{\mu\nu}) \epsilon^{\mu\nu\alpha\beta} (B_{\alpha\beta} + F_{\alpha\beta}) + \frac{1}{12\Lambda^2} H_{\mu\nu\alpha} H^{\mu\nu\alpha}. \quad (6)$$

Since fields enter only in the combination  $(B_{\mu\nu} + F_{\mu\nu})$ , the gauge invariance of the second kind of  $B_{\mu\nu}$  is ensured by the simultaneous shift  $A_\mu \rightarrow A_\mu - \lambda_\mu$ , leading to three degrees of freedom of mass, see Methods,

$$m_\theta = \frac{f\Lambda}{4\pi} \sqrt{\left(\frac{4\pi}{f^2}\right)^2 + \left(\frac{\theta}{\pi}\right)^2}. \quad (7)$$

Two of them belong in the original gauge field and one is from the new field due to the monopole condensate. Alternatively, the original electromagnetic field tensor  $F_{\mu\nu}$  can be reabsorbed by the new field in a generalized Stückelberg mechanism [36] dual to the familiar Anderson-Higgs mechanism. The Stückelberg mechanism is the Anderson-Higgs mechanism without a Higgs field or, in other words, the limit of



the Anderson-Higgs mechanism in which the Higgs field becomes infinitely heavy and predates both the Anderson and the Higgs versions. When in condensed matter applications, one finds the combination  $(\partial_\mu \varphi - A_\mu)$  for the phase of the order parameter and the gauge field, one is actually speaking of the Stückelberg mechanism, much anterior to Andersons realization. Usually, it is the photon that “eats up the phase of the order parameter. Here, in its dual formulation, in which the scalar is encoded in the antisymmetric tensor field, it is the opposite. To conclude here, the electromagnetic response of the oblique superinsulator expresses fully in terms of the antisymmetric tensor field with three degrees of freedom and mass (7).

The mass (7) is the sum of normal and topological contributions. In the limit  $f \gg 1$ , the topological contribution dominates and the mass eventually diverges as  $f \rightarrow \infty$ ,  $\Lambda \rightarrow \infty$ . In this limit, the bulk dynamics is frozen because only the topological contribution,

$$\mathcal{L}_{\text{top}} = \frac{\theta}{32\pi^2} (B_{\mu\nu} + F_{\mu\nu}) \epsilon^{\mu\nu\alpha\beta} (B_{\alpha\beta} + F_{\alpha\beta}), \quad (8)$$

survives in the Lagrangian. The topological regime is realized deep in the underdoped region, where  $f \gg 1$ .

Let us now consider the oblique superinsulator on an open manifold  $M$  with the boundary  $\partial M$ . The fields  $B_{\mu\nu}$  and  $A_\mu$  in Eq. (6) contain transverse and longitudinal modes, the latter being encoded in the gauge field  $\lambda_\mu$  defined by  $B_{\mu\nu} = \partial_\mu \lambda_\nu - \partial_\nu \lambda_\mu$  and the scalar  $\xi$  defined by  $A_\mu = \partial_\mu \xi$ . In the topological limit the mass (7) diverges and all bulk transverse modes get frozen. The longitudinal modes, however, contribute a total derivative into Eq. (8). When the model is defined on a bounded space, this total derivative for the longitudinal modes is all that remains and it gives rise to a boundary theory governed by the Lagrangian

$$\mathcal{L}_{\partial M} = \frac{\theta}{8\pi^2} \lambda_\mu \epsilon^{\mu\alpha\gamma} \partial_\alpha \lambda_\gamma + \frac{\theta}{2\pi} \lambda_\mu \Phi^\mu - \frac{M}{2} v^2 (\partial_i \xi)^2 - \frac{\theta^2}{2\pi^2 M} b^2 \quad (9)$$

$$= \frac{\theta}{8\pi^2} \lambda_\mu \epsilon^{\mu\alpha\gamma} \partial_\alpha \lambda_\gamma + \frac{\theta}{2\pi} \lambda_0 \Phi^0 - \frac{\theta}{\pi} b \dot{\xi} - \frac{M}{2} v^2 (\partial_i \xi)^2 - \frac{\theta^2}{2\pi^2 M} b^2, \quad (10)$$

where  $\Phi^\mu = (1/2\pi) \epsilon^{\mu\alpha\beta} \partial_\alpha \partial_\beta \xi$  represents the vortex current and  $b = (1/2\pi) \epsilon^{ij} \partial_i \lambda_j$  plays the role of the “charge” canonically conjugate to the phase  $\xi$ . The kinetic terms for the surface modes are added-in a posteriori and, correspondingly  $M$  is a non-universal mass scale and  $v$  is the non-universal propagation speed of the surface modes.

The Hamiltonian of the boundary theory is derived by setting the canonical momenta  $\pi_\xi = -(\theta/\pi)b$  and  $\pi_{\lambda_2} = -(\theta/4\pi^2)\lambda_1$  (as usual in pure Chern-Simons theories, one has a choice of deciding which of two components assumes the role of the coordinate and which one is the momentum). Setting the Lagrange multiplier  $\lambda_0 = 0$  (Weyl gauge) and writing down the Gauss law constraint,  $b = -\Phi^0$ , it implements, one arrives at

$$\mathcal{H}_{\partial M} = \frac{1}{2M} \pi_\xi^2 + \frac{M}{2} v^2 (\partial_i \xi)^2, \quad (11)$$

which describes a massless degree of freedom. The corresponding Hamilton equation of motion is  $(\partial_0^2 - v^2 \sum_i \partial_i^2) \xi = 0$ . The gauge field  $\lambda_\mu$  is not a dynamical field because there are no “electric fields” appearing in the Lagrangian, and it is expressed entirely in terms of the vortex configuration via the Chern-Simons Gauss law constraint [38]. This constraint,  $b = -\Phi^0$ , implies that the momentum  $\pi_\xi$  conjugate to the phase  $\xi$  is not an electric charge, as it would be in superconductors, but the vortex number itself. However, these boundary vortices carry also unit electric charge ( $2e$ ), as can be seen by including the electromagnetic coupling  $(\theta/2\pi) A_\mu \Phi^\mu$ . They are

thus dyons themselves. Finally, it follows from the formulation (9) of the boundary Lagrangian, that these dyons acquire fractional statistics via the boundary Chern-Simons term [39]. In particular, for the relevant case  $\theta = 2\pi$  they become fermions. Thus, the topological limit of the oblique superinsulators for  $\theta = 2\pi$  contains only boundary states which are massless fermionic dyons carrying unit magnetic and electric charges. The canonical structure and the massless character of these boundary fermions rests on the U(1) combined gauge symmetry  $\lambda_\mu \rightarrow \lambda_\mu + \partial_\mu \chi$  and  $\xi \rightarrow \xi - \chi$  inherited from the bulk. Any boundary perturbation that leaves this symmetry intact does not affect the dynamics of the boundary fermions, which are symmetry-protected surface states. Boundary perturbations that break time-reversal symmetry can affect their statistics by effectively changing the value of  $\theta$ . As a consequence, these surface fermions behave as a Fermi liquid.

## DISCUSSION

The developed theory provides a consistent, unified insight into the observed universal properties of the pseudogap and adjacent phases emerging near the tricritical point. First, the characteristic resistivity  $\rho \propto T^2$  of the pseudogap state [1] arises from the Fermi-liquid behaviour of the symmetry-protected surface fermions in the dyon conden-

sate. These are intimately associated with the presence of the  $\theta$ -term in the electromagnetic response, eq. (1), which naturally explains the onset of magnetoelectric effects in the pseudogap state, exactly as in strong topological insulators, see [40]. The observation that superconducting fluctuations and quantum correction contributions to the resistive behavior near the dome is perfectly well described by the standard 2D formulas, see for example, [41, 42], indicates that the parameters of the boundary fermions are close to those of the standard normal quasiparticle excitations in the corresponding materials. The fact that the structurally simple model compound Hg1201 exhibits negligible residual resistivity [1] complies perfectly well with the notion that for the symmetry-protected 2D boundary fermions localization is absent. Importantly, while the cuprates exhibit quasi-2D physics, the dyon condensate responsible for HTS properties and the phase diagram structure is essentially of three-dimensional origin. This seeming contradiction is immediately resolved by the fact that the two adjacent CuO planes that present the unit cell of cuprates are enough to ensure the existence of Dirac monopoles and the 3D-like interaction between monopoles and Cooper pairs. This explains why even a few- and monolayer cuprates may exhibit practically the same superconducting transition temperature  $T_c$  as bulk samples [18, 42].

Turning to the detailed Hall resistance experimental data [43], we recall that, in optimally doped cuprates, the sign reversal of the Hall resistance is attributed to the contribution of vortices carrying in the core excessive electric charge [42, 44]. It is natural to conjecture that, in the underdoped regime in the vicinity of the quantum critical point marking the onset of the superconducting dome, dyons that carry both electric and magnetic charge take up on the role of vortices with excessive electric charge. Moreover, recalling further that the data on the charge Berezinskii-Kosterlitz-Thouless transition into the superinsulating state [45] indicate that the boundary fermionic states are harbored by the percolation Chalker-Coddington structure, which is known to be a natural host for gapless boundary states [46], one naturally expects erratic behavior with noticeable random components, exactly as observed in the experiment [43]. However, further theoretical study of the dyon-related Hall effect for a quantitative description of the experiment is needed.

The underdoped antiferromagnetic phase of the cuprates holding exactly a single hole per Cu site perfectly realizes a 2D spin square Heisenberg antiferromagnet, and the symmetry of the lattice is thus  $C_4$ . In such a lattice the adjacent spins are opposite while the diagonal ones are parallel. As a result, the combined electric/magnetic symmetry of the lattice reduces to  $C_2$ . Since the boundary fermion are dyons (due to the  $\theta$ -term) and carry thus both electric and magnetic charge they feel the combined  $C_2$  symmetry, hence nematicity with the nematic director pointing in the direction of the CuO lattice diagonals, which is an essential characteristic of the PG state [3, 8] going hand-in-hand with the  $T^2$  resistance.

Finally, we turn to the discussion of the linear,  $R_\square \propto T$ , resistance behavior in the overdoped region, observed at high

magnetic fields, sufficient to destroy the Cooper pair condensate, and low temperatures. This has been recently declared a major puzzle of condensed-matter physics [47]. Its generic character in HTS is established experimentally and is associated with a universal scattering rate, the origin of which remains a mystery. A careful experimental analysis [48] reveals that the slopes of the linear terms in the low-temperature regime and in the high-temperature, inherently metallic phase, are substantially different. Moreover, at sufficiently low temperatures and high magnetic field  $B$  there is an intercept which is also linear in  $B$  [48], so that the resistivity assumes the form  $\rho = aT + bB$ . These two can be considered as thermal and quantum contributions, respectively. The resolution of the linear in  $T$  puzzle lies in the fact that, in the presence of magnetic monopoles, the out-of-condensate Cooper pairs behave as fermions [33, 34]. At low temperatures, these fermions scatter primarily with bogolons, the coherent fluctuations of the residual dyon condensate domains [49]. At temperatures higher than the Bloch-Grüneisen temperature  $T_{BG} \approx 2sk_F/k_B$ , where  $k_F$  is the Fermi momentum of the fermionic Cooper pairs and  $s$  is the sound velocity of the bogolons, the resistance due to this scattering mechanism is linear in  $T$ ,  $R_\square \propto T$  [49]. Let us recall that in HTS the zero-temperature superfluid density  $n_s$ , and, accordingly, the effective ‘Fermi energy,’  $\epsilon_F^* \approx n_s \xi / 4m^*$ , associated with fermionic Cooper pairs is relatively low [50],  $\xi$  is the superconducting coherence length, and  $m^*$  is the effective mass of the carriers. Accordingly, the Bloch-Grüneisen temperature  $T_{BG}$  is low, especially if the bogolon sound velocity  $s$  is also small. Thus, the universal scattering time  $\tau \sim \hbar/k_B T$  (in physical units) for  $T > T_{BG}$  arises similarly to the usual high temperature electron-phonon scattering time. To understand the origin of the different slopes at low and high temperatures, note that the linear dependence can be understood in the framework of the Anderson orthogonality catastrophe (AOC) approach. Indeed, one expects that all the relevant microscopic times are shorter than the scattering time  $\tau$ . According to the AOC,  $\tau$  is related to the heat,  $Q$ , generated by the scattering processes by the universal relation [51]  $\hbar/\tau = fQ$ , where  $f \approx O(1)$  is some numerical function of the microscopic parameters. Adopting  $Q = k_B T \delta S$ , where  $\delta S$  is the entropy change associated with the scattering and weakly (logarithmically) depending on temperature [51], one arrives at the universal relation  $1/\tau = \alpha k_B T / \hbar$ ,  $\alpha = O(1)$ , giving rise to the linear-in- $T$  resistivity. Since the microscopic origin of the scattering at high and low temperatures is different, one has to expect the different scattering-related entropy changes, hence different slopes.

Turning to the effect of strong magnetic fields, we note that in the high field limit, the number of available degenerate ground states occupied by bosons in the area  $A$  perpendicular to magnetic field  $B$  is  $N = (1/2\pi)(eB/\hbar)$  (see, e.g. [52]). This is the number of available scattering centres at  $T = 0$  and the same reasoning that leads to the linear-in- $T$  resistance leads to the observed linear-in- $B$  behaviour of the intercept. In other words, at high fields the role of the temperature  $T$  is taken by  $\hbar\omega_c$ , where  $\omega_c = eB/m^*c$  is the cyclotron frequency [53].

A final comment is in order. As we have mentioned above, the boundary fermionic states are harbored by the percolation Chalker-Coddington structure in accord with experimental findings of [43]. It implies that one can identify  $T^*$  with the temperature at which the "bubbles" hosting massless boundary dyon states form finite clusters but do not extend across the whole system. Then the  $T^{**}$  line in the phase diagram is the line of the percolation transition at which the Chalker-Coddington structure spreads across the system and the pseudogap state with nematicity, the  $T^2$  resistance and magneto-electric effects is fully formed.

### Acknowledgments

M. C. D. thanks CERN, where she completed this work, for kind hospitality. The work at Argonne (V.M.V.) was supported by the U.S. Department of Energy, Office of Science, Materials Sciences and Engineering Division.

### APPENDIX

#### Lattice BF term

To formulate the gauge-invariant lattice  $BF$ -term, we follow [12] and introduce the lattice  $BF$  operators

$$K_{\mu\nu\rho} \equiv S_\mu \epsilon_{\mu\alpha\nu\rho} \Delta_\alpha, \quad \hat{K}_{\mu\nu\rho} \equiv \epsilon_{\mu\nu\alpha\rho} \hat{\Delta}_\alpha \hat{S}_\rho, \quad (12)$$

where

$$\begin{aligned} \Delta_\mu f(x) &\equiv f(x + \ell \hat{\mu}) - f(x), \quad S_\mu f(x) \equiv f(x + \ell \hat{\mu}), \\ \hat{\Delta}_\mu f(x) &\equiv f(x) - f(x - \ell \hat{\mu}), \quad \hat{S}_\mu f(x) \equiv f(x - \ell \hat{\mu}), \end{aligned} \quad (13)$$

are the forward and backward lattice derivative and shift operators, respectively. Summation by parts on the lattice interchanges both the two derivatives (with a minus sign) and the two shift operators; gauge transformations are defined using the forward lattice derivative. The two lattice  $BF$  operators are interchanged (no minus sign) upon summation by parts on the lattice and are gauge invariant in the sense that

$$\begin{aligned} K_{\mu\nu\rho} \Delta_\nu &= K_{\mu\nu\rho} \Delta_\rho = \hat{\Delta}_\mu K_{\mu\nu\rho} = 0, \\ \hat{K}_{\mu\nu\rho} \Delta_\rho &= \hat{\Delta}_\mu \hat{K}_{\mu\nu\rho} = \hat{\Delta}_\nu \hat{K}_{\mu\nu\rho} = 0. \end{aligned} \quad (14)$$

They also satisfy the equations

$$\begin{aligned} \hat{K}_{\mu\nu\rho} K_{\rho\lambda\omega} &= -(\delta_{\mu\lambda} \delta_{\nu\omega} - \delta_{\mu\omega} \delta_{\nu\lambda}) \nabla^2 \\ &+ (\delta_{\mu\lambda} \Delta_\nu \hat{\Delta}_\omega - \delta_{\nu\lambda} \Delta_\mu \hat{\Delta}_\omega) + (\delta_{\nu\omega} \Delta_\mu \hat{\Delta}_\lambda - \delta_{\mu\omega} \Delta_\nu \hat{\Delta}_\lambda), \end{aligned} \quad (15)$$

$$\hat{K}_{\mu\nu\rho} K_{\rho\nu\omega} = K_{\mu\nu\rho} \hat{K}_{\rho\nu\omega} = 2(\delta_{\mu\omega} \nabla^2 - \Delta_\mu \hat{\Delta}_\omega), \quad (16)$$

where  $\nabla^2 = \hat{\Delta}_\mu \Delta_\mu$  is the lattice Laplacian.

### Finite Temperature Deconfinement Transition

In field theory, a finite temperature  $T$  is introduced by formulating the action on a Euclidean time of finite length  $\beta = 1/T$ , with periodic boundary conditions (we have reabsorbed the Boltzmann constant into the temperature). If the original field theory model is defined on a Euclidean lattice of spacing  $\ell$ , then  $\beta$  is quantized in integer multiples of  $1/\ell$  as  $\beta = b/\ell$ , with  $b$  an integer.

The lattice Coulomb Green's function  $G(0)$  at coinciding points is

$$G(0) = \frac{1}{(2\pi)^4} \int_{-\pi}^{\pi} d^4 k \frac{1}{\sum_{i=0}^3 4 \sin\left(\frac{k_i}{2}\right)^2}. \quad (17)$$

At finite temperatures,  $k^0$  is both defined on a Brillouin zone of length  $2\pi$  and also invariant under shifts  $k^0 \rightarrow k^0 + 2\pi/\ell\beta$ . This can be achieved only by introducing integers  $k \in [-b, b]$ , called Matsubara frequencies, and restrict the allowed values to  $k^0 = \pi k/b$ . Correspondingly, integrals over  $k^0$  have to be replaced by sums over Matsubara frequencies,

$$\int_{-\pi}^{\pi} dk^0 f(k^0) \rightarrow \sum_{k=-b}^{k=b} \frac{\pi}{\beta} f\left(\frac{\pi k}{b}\right). \quad (18)$$

As a consequence, at finite temperatures  $G(0)$  becomes

$$G(0, T) = \frac{1}{(2\pi)^4} \sum_{k=-b}^{k=b} \frac{\pi}{b} \int_{-\pi}^{\pi} \frac{dk^1 dk^2 dk^3}{4 \sin\left(\frac{\pi k}{2b}\right)^2 + \sum_{i=1}^3 4 \sin\left(\frac{k_i}{2}\right)^2}. \quad (19)$$

This affects primarily the parameter  $\eta$  which becomes a function of the temperature,  $\eta(T) = \pi G(0, T)/\mu$ . Introducing the scale function  $S(T) = \sqrt{G(0)/G(0, T)}$  we obtain the result that, at finite temperatures the overall scale of the ellipse (5) shrinks by  $S(T)$ ,  $\sqrt{1/\eta} \rightarrow S(T) \sqrt{1/\eta}$ .

### Topological two-form mass term in 3D

Let us consider the following model for an antisymmetric tensor  $b_{\mu\nu}$  in 3D [36]

$$\mathcal{L} = \frac{1}{12\Lambda^2} h_{\mu\nu\alpha} h^{\mu\nu\alpha} - \frac{1}{4f^2} b_{\mu\nu} b^{\mu\nu} + \frac{\theta}{32\pi^2} b_{\mu\nu} \epsilon^{\mu\nu\alpha\beta} b_{\alpha\beta}, \quad (20)$$

where  $h_{\mu\nu\alpha} = \partial_\mu b_{\nu\alpha} + \partial_\nu b_{\alpha\mu} + \partial_\alpha b_{\mu\nu}$  is the three-form field strength,  $\Lambda$  has dimension [mass] and  $f$  and  $\theta$  are dimensionless. The first two terms are the generalization to two forms of the Proca Lagrangian for a massive vector field. The third term is topological, since it is metric-independent.

The equations of motions of this model are

$$\partial_\mu h^{\mu\alpha\beta} + \frac{\Lambda^2}{f^2} b^{\alpha\beta} - \frac{\Lambda^2 \theta}{8\pi^2} \epsilon^{\alpha\beta\gamma\delta} b_{\gamma\delta} = 0. \quad (21)$$

Contracting with  $\partial_\alpha$  we obtain the condition

$$\partial_\mu b^{\mu\nu} + \frac{f^2\theta}{4\pi^2} h^\nu = 0, \quad (22)$$

where  $h^\mu = (1/6)\epsilon^{\mu\nu\alpha\beta}h_{\nu\alpha\beta}$  is the dual field strength. Finally, contracting (21) with  $\epsilon_{\gamma\nu\alpha\beta}\partial^\gamma$  and using the above condition we get

$$(\partial^2 + m_\theta^2)h^\mu = 0, \quad m_\theta = \frac{f\Lambda}{4\pi} \sqrt{\left(\frac{4\pi}{f^2}\right)^2 + \left(\frac{\theta}{\pi}\right)^2}. \quad (23)$$

This shows that there is a topological contribution to the mass.

## DATA AVAILABILITY

Data sharing not applicable to this article as no datasets were generated or analyzed during the current study.

- 
- [1] Barišić, N. *et al.* Universal sheet resistance and revised phase diagram of the cuprate high-temperature superconductors. *PNAS* **110**, 12235 – 12240 (2013).
  - [2] Keimer, B., Kivelson, S. A., Norman, M. R., Uchida, S. & Zaanen, J. From quantum matter to high-temperature superconductivity in copper oxides. *Nature* **518**, 179186 (2015).
  - [3] Sato, Y. *et al.* Thermodynamic evidence for a nematic phase transition at the onset of the pseudogap in YBa<sub>2</sub>Cu<sub>3</sub>O<sub>y</sub>. *Nature Physics* **13**, 1074 – 1078 (2017).
  - [4] Zhou, P. *et al.* Electron pairing in the pseudogap state revealed by shot noise in copper oxide junctions. *Nature* **572**, 493 (2019).
  - [5] Proust, C. & Taillefer, L. The Remarkable Underlying Ground States of Cuprate Superconductors. *Annu. Rev. Condens. Matter Phys.* **10**, 409 – 429 (2019).
  - [6] Proust, C., Vignolle, B., Levallois, J., Adachi, S. & Hussey, N. E. Fermi liquid behavior of the in-plane resistivity in the pseudogap state of YBa<sub>2</sub>Cu<sub>4</sub>O<sub>8</sub>. *PNAS* **113**, 13564 – 13659 (2016).
  - [7] Mukhopadhyay, S. *et al.* Evidence for a vestigial nematic state in the cuprate pseudogap phase. *PNAS* **116**, 13249 – 13254 (2019).
  - [8] Kivelson, S. A., Fradkin, E. & Emery, V. J. Electronic liquid-crystal phases of a doped Mott insulator. *Nature*, **393**, 550553 (1998).
  - [9] Nie, L., Tarjus, & Kivelson, S. A. Quenched disorder and vestigial nematicity in the pseudogap regime of the cuprates. *PNAS*, **111**, 7980 – 7985 (2014).
  - [10] Zheng, G. Q., Kuhns, P. L., Reyes, A. P., Liang, B. & Lin, C. T. Critical point and the nature of the pseudogap of single-layered copper-oxide Bi<sub>2</sub>Sr<sub>2-x</sub>La<sub>x</sub>CuO<sub>6+δ</sub> superconductors. *Phys. Rev. Lett.* **94**, 047006 (2005).
  - [11] Goldman, A. M. Superconductor-insulator transitions. *Int. J. Mod. Phys. B* **24** 4081-4101 (2010).
  - [12] Diamantini M. C., Sodano, P. & Trugenberger, C. A. Gauge theories of Josephson junction arrays. *Nuclear Physics B* **474**, 641 – 677 (1996).
  - [13] Das, D. & Doniach, S. Existence of a Bose metal at  $T = 0$ . *Phys. Rev. B* **60**, 1261 – 1275 (1999).
  - [14] Kapitulnik, A., Kivelson, S. A. & Spivak, B. Anomalous metals – failed superconductors. *Rev. Mod. Phys.* **91**, 011002 (2019).
  - [15] Diamantini, M. C. *et al.* Bose topological insulator intermediate state in the superconductor-insulator transition. *Phys. Lett. A* **384** 126570 (2020).
  - [16] Lu, Y.-M. & Vishwanath, A. Theory and Classification of interacting integer topological phases in two dimensions: a Chern-Simons approach. *Phys. Rev B* **86**, 125119 (2012).
  - [17] Chen, X., Gu, Z.-C., Liu, Z.-X. & Wen, X.-G. Symmetry protected topological orders and the group cohomology of their symmetry group. *Phys. Rev. B* **87**, 155114 (2013).
  - [18] Yu, Y. *et al.* High-temperature superconductivity in monolayer Bi<sub>2</sub>Sr<sub>2</sub>CaCu<sub>2</sub>O<sub>8+δ</sub>. *Nature* **575**, 156 – 163 (2019).
  - [19] Vishwanath, A. & Senthil, T. Physics of Three-Dimensional Bosonic Topological Insulators: Surface-Deconfined Criticality and Quantized Magnetoelectric Effect. *Phys. Rev. X* **3** 011016 (2013).
  - [20] Vinokur, V. M. *et al.* Superinsulator and quantum synchronization. *Nature* **452**, 613 – 615 (2008).
  - [21] Polyakov, A. Compact gauge fields and the infrared catastrophe. *Physics Letters B* **59**, 82-84 (1975).
  - [22] Goddard, P. & Olive, D. I. Magnetic monopoles in gauge fields theories, *Rep. Progr. Phys.* **41**, 1357-1437 (1978).
  - [23] Trugenberger, C. A., Diamantini, M. C., Poccia, N., Nogueira, F. S. & Vinokur, V. M. Magnetic monopoles and superinsulation in Josephson junction arrays. *Quantum Reports* **2**, 388 – 399 (2020); <http://dx.doi.org/10.3390/quantum2030027>.
  - [24] Diamantini, M. C., Trugenberger, C. A. & Vinokur, V. M. Quantum magnetic monopole condensate. In press.
  - [25] Diamantini, M. C., Trugenberger, C. A. & Vinokur, V. M. Confinement and asymptotic freedom with Cooper pairs. *Comm. Phys.* **1**, 77 (2018).
  - [26] Diamantini, M. C., Gamaitoni, L., Strunk, C., Postolova, S. V., Mironov, A. Yu., Trugenberger, C. A. & Vinokur, V. M. Direct probe of the interior of a meson. arXiv:1906.12265.
  - [27] Wilczek, F. Two applications of axion electrodynamics. *Phys. Rev. Lett.* **58**, 1799 (1987).
  - [28] Cardy, J. L. & Rabinovici, E. Phase structure of Z(p) models in presence of theta parameter. *Nucl. Phys. B* **205**, 1-16 (1982).
  - [29] Witten, E. Dyons of Charge  $2\theta/2\pi$ . *Phys. Lett.* **86**, 283-287 (1979).
  - [30] Banks, T., Myerson, R. & Kogut, J. Phase transitions in Abelian lattice gauge theories. *Nucl. Phys. B* **129**, 493-510 (1977).
  - [31] 't Hooft, G. Topology of the gauge condition and new confinement phases in non-Abelian gauge theories. *Nucl. Phys. B* **190**, 455-478 (1981).
  - [32] Metlitski, M. A., Kane, C. L. & Fisher, M. P. A. Bosonic topological insulator in three dimensions and the statistical Witten effect. *Phys. Rev. B* **88**, 035131 (2013).
  - [33] Jackiw, R. & Rebbi, C. Spin from isospin in a gauge theory. *Phys. Rev. Lett.* **36**, 1116 (1976).
  - [34] Hasendfratz, P. & 't Hooft, G. A fermion-boson puzzle in a gauge theory. *Phys. Rev. Lett.* **36**, 1119 (1976).
  - [35] Goldhaber, A. S., MacKenzie, R. & Wilczek, F. Field corrections to induced statistics. *Mod. Phys. Lett.* **4**, 21-31 (1989).
  - [36] Quevedo, F. & Trugenberger, C. A. Phases of antisymmetric tensor field theories. *Nucl. Phys. B* **501**, 143-172 (1997).
  - [37] Diamantini, M. C., Quevedo, F. & Trugenberger, C. A. Confining Strings with Topological Term. *Phys. Lett. B* **396**, 115 – 121 (1997).
  - [38] Jackiw, R. Topics in planar physics. in *Physics, Geometry and Topology*, H. C. Lee ed. Plenum Press, New York (1989).
  - [39] Wilczek, F. *Fractional statistics and anyon superconductivity*. World Scientific, Singapore (1990).



- [40] Essin, A. M., Moore, J. E. & Vanderbilt, D. Magnetoelectric Polarizability and Axion Electrodynamics in Crystalline Insulators. *Phys. Rev. Lett.* **102**, 146805 (2009).
- [41] Pomar, A., Ramallo, M. V., Mosqueira, J., Torrón, C. & Vidal, F. Fluctuation-induced in-plane conductivity, magnetoconductivity, and diamagnetism of  $\text{Bi}_2\text{Sr}_2\text{CaCu}_2\text{O}_8$  single crystals in weak magnetic fields. *Phys. Rev. B* **54**, 7470 – 7480 (1996).
- [42] Zhao, F. *et al.* Sign-Reversing Hall Effect in Atomically Thin High-Temperature  $\text{Bi}_{2.1}\text{Sr}_{1.9}\text{CaCu}_{2.0}\text{O}_{8+\delta}$  Superconductors. *Phys. Rev. Lett.* **122**, 247001 (2019).
- [43] Wu, J., Bollinger, A. T., Sun Y. & Bozovic I. Hall effect in quantum critical charge-cluster glass, *PNAS* **113** 4284-4289 (2016).
- [44] Feigelman, M. V., Geshkenbein, V. B., A. I. Larkin, A. I. & Vinokur, V. M. Sign change of the flux-flow Hall effect in HTSC. *JETP Lett.* **62**, 834 – 837 (1995).
- [45] Mironov, A. Yu. *et al.* Charge Berezinskii-Kosterlitz-Thouless transition in superconducting NbTiN films. *Scientific Reports* **8** 4082 (2018).
- [46] Ochiai, T. Gapless surface states in a three-dimensional Chalker-Coddington type network model. <http://arxiv.org/abs/1510.04033v1> (2015).
- [47] Legros, A. *et al.* Universal T-linear resistivity and Planckian dissipation in overdoped cuprates. *Nature Physics* **15**, 142 – 147 (2019).
- [48] Giraldo-Gallo P. *et al.* Scale-invariant magnetoresistance in a cuprate superconductor. *Science* **361**, 479-481 (2018).
- [49] Sun, M., Villegas, K. H. A., Kovalev V. M., & Savenko G., Bogolon-mediated electron scattering in graphene and hybrid Bose Fermi systems. *Phys. Rev. B* **99** 115408 (2019).
- [50] Emery, V. J. & Kivelson, S. A. Importance of phase fluctuations in superconductors with small superfluid density. *Nature* **374**, 434 – 437 (1995).
- [51] Lebedev, A. V. & Vinokur, V. M. Heat generation due to Anderson catastrophe in mesoscopic devices. *Phys. Rev. B*, in press.
- [52] Abrikosov, A. A. Fundamentals of the Theory of Metals. *North Holland, Amsterdam*, 1988.
- [53] Glatz, A., Varlamov, A. A. & Vinokur, V. M. Fluctuation spectroscopy of disordered two-dimensional superconductors. *Phys. Rev. B* **84**, 104510 (2011).